© Pol J Radiol 2023; 88: e455-e460
DOI: https://doi.org/10.5114/pjr.2023.131911

Received: 17.07.2023
Accepted: 26.08.2023
Published: 04.10.2023

Polish Journal of Radiology

http://www.polradiol.com

Original paper

Application of diffusion kurtosis imaging in differential diagnosis of focal liver lesions

Joanna Podgórska[1,2,A,B,C,D,E,F], Katarzyna Pasicz[3,A,B,C,D,E,F], Witold Skrzyński[3,A,B,C,D,E,F], Bogumił Gołębiewski[2,B], Piotr Kuś[2,B], Jakub Jasieniak[2,A,B,C,D], Agnieszka Rogowska[4,5,A,B], Paweł Kukołowicz[3,A,D,E], Andrzej Cieszanowski[1,2,A,B,D,E]

[1]2nd Department of Clinical Radiology, Warsaw Medical University, Poland
[2]Department of Radiology 1, the Maria Sklodowska-Curie National Research Institute of Oncology, Warsaw, Poland
[3]Department of Medical Physics, the Maria Sklodowska-Curie National Research Institute of Oncology, Warsaw, Poland
[4]Department of Gastroenterology, Hepatology and Clinical Oncology, Centre of Postgraduate Medical Education, Warsaw, Poland
[5]Department of Oncological Gastroenterology, the Maria Sklodowska-Curie National Research Institute of Oncology, Warsaw, Poland

Abstract

Purpose: Diffusion kurtosis imaging (DKI) is an MRI method related to diffusion imaging (DWI) that is distinguished by a non-Gaussian calculation of water particles movements in tissues. The aim of the study was to assess DKI advantage over DWI in differentiating benign and malignant liver lesions.

Material and methods: Analysis included prospectively acquired group of 83 patients referred consecutively for 3T-MRI liver tumor examination, with 95 liver lesions (31 benign, 59 malignant). MRI assessments were performed with standard protocol and DKI sequence with seven *b*-values (0-2,000 s/mm^2). Quantitative data were acquired by placing ROIs in liver tumors on all *b*-value images, ROI data extracted, and calculation of DWI and DKI parameters. ADC was calculated for all *b*-values ($ADC_{0\text{-}2000}$) and for three values of b = 0, 500, and 750 (s/mm^2) ($ADC_{0\text{-}500\text{-}750}$). DKI and ADC parameters for benign and malignant lesions were compared, and ROC curves were plotted.

Results: Significant differences were obtained for all DKI and ADC parameters. ROC analysis showed AUC of D_K, K, $ADC_{0\text{-}2000}$, and $ADC_{0\text{-}500\text{-}750}$ was 0.74, 0.77, 0.77, and 0.75, respectively. The highest sensitivity (of 0.91) was obtained for $ADC_{0\text{-}2000}$. The highest specificity (0.65) and accuracy (0.80) was obtained for K.

Conclusion: DKI technique yields statistically comparable results with DWI technique.

Key words: MRI, diffusion kurtosis imaging (DKI), diffusion weighted imaging (DWI), liver tumor.

Introduction

Diffusion kurtosis imaging (DKI) is an MRI method related to diffusion imaging (DWI) evaluated by a non-Gaussian approach to calculate diffusion of water in tissues. The theoretical basis emphasizing this method, as reported by Jensen *et al.* [1], is an assumption that non-Gaussian analysis can reveal the presence of natural barriers in tissues, such as cell membranes and organelles, implying an advantage over the Gaussian diffusion model applied in DWI. However, for differences between the two models, it is necessary to acquire ultra-high values of *b*-value (> 1,000 s/mm^2).

DKI has been analyzed in several studies to detect and stage liver fibrosis [2]. While many papers have concentrated on different aspects of hepatocellular carcinoma (HCC) [3-7],

Correspondence address:
Joanna Podgórska, 2nd Department of Clinical Radiology, Warsaw Medical University, Warsaw, Poland, phone: +48-22-599-2300, e-mail: jpodgo@gmail.com

Authors' contribution:
A Study design · **B** Data collection · **C** Statistical analysis · **D** Data interpretation · **E** Manuscript preparation · **F** Literature search · **G** Funds collection

only limited studies have focused on the differentiation of liver focal lesions. In regard to malignant liver lesions being distinguished from benign ones, we were able to find two studies only. Jia et al. showed that ADC- and DKI-derived parameters allow HCC to be differentiated from focal nodular hyperplasia (FNH), hemangioma, and HCA; however, metastases were not included in that study [4]. In turn, in a study performed by Budjan *et al*., a standard DWI protocol with the highest *b*-value of 1,000 s/mm^2 was applied in calculating DKI parameters [8], though in line with the method's concept, it would be beneficial to apply still-higher values (up to *b*-value = 2,000 s/mm^2).

On that basis, in the present paper, we sought to assess whether DKI applying ultra-high b-values may have an advantage over DWI technique in differentiating benign and malignant liver lesions.

Material and methods

Study population

The study protocol was approved by the local ethics committee (Bioethical Commission at the Maria Sklodowska-Curie National Research Institute of Oncology; approval number 11/2017), and informed consent was obtained from all patients prior to examination. Between 2017 and 2020, the study group was acquired prospectively, and consisted of 83 patients (female, *n* = 45; male, *n* = 38; age range, 23-85 years; median age, 61 years) referred consecutively for MRI of the liver due to suspected liver tumor. Criteria for inclusion were age over 18, a suspicious liver mass, no prior oncological treatment, and consent to participate in the study. Exclusion criteria were contraindications to MRI. Within the cohort, a total of 95 liver lesions were found, of which 31 were diagnosed as benign (9 FNH, 4 regenerative nodules [RN], and 18 hemangiomas), while 59 lesions were malignant (11 intra-hepatic cholangiocarcinomas [iCCA], 10 HCCs, and 38 metastases). The diagnosis of benign lesions was based on typical MRI characteristics and 12-44 months of follow-up.

Table 1. Acquisition parameters for diffusion kurtosis imaging (DKI) sequence applied

T_R (repetition time)	7,400 ms
T_E (echo time)	67 ms
Number of slices	33
Slice thickness	5 mm
Echo spacing	0.54 ms
Number of gradient directions	3
Filter	Moderate
Distortion correction	On
Bandwidth	2332 Hz/px
NSA	1-8

In malignant masses, 6 HCCs were diagnosed on the basis of LI-RADS criteria (LR5 lesions) [9], whereas in remaining lesions, the diagnosis was based on biopsy and histopathological examination.

MRI protocol

MRI examinations were performed on a 3T MR system (MAGNETOM Skyra, Siemens Healthcare, Erlangen, Germany), with an 18-channel phased array body coil in combination with a 32-channel spine coil. Within a standard liver tumor diagnosis in MRI protocol, a spin-echo echo-planar DKI sequence was done, with acquisition of seven *b*-values, including 0, 200, 500, 750, 1,000, 1,500, and 2,000 s/mm^2 in the axial plane. Details of the DKI sequence are shown in Table 1. The remainder of protocol consisted of sequences T2 HASTE, T2 HASTE fs, T2 TSE fs, Trufisp, VIBE Dixon, CE Twist VIBE Dixon with 70 min delayed phase after administration of hepatobiliary contrast (Multihance, Bracco Imaging Deutschland GmbH, Germany).

Image analysis

Image analysis were obtained using a scanner dedicated workstation, syngo.via (Siemens Healthcare, Erlangen, Germany). Quantitative data were acquired by three board-certified radiologists (JP, PK, and BG). Regions of interest (ROIs) were located in each liver tumor on a *b*-value = 750 image, with regions of necrosis or hemorrhage avoided. The regions were copied to all DKI *b*-value images, with ROIs data (mean signal intensity [SI] and standard deviation [SD]) extracted for further analysis.

Calculation of DWI and DKI parameters

The calculation of parameters was achieved with GNUPLOT software (version 5.0, patch level 4), while function fitting was done using a non-linear least squares (NLLS) Marquardt-Levenberg algorithm.

The respective formula used in calculating DKI and ADC parameters were as follow:

$$\ln [S(b)/S(0)] = -b \times D_K + 1/6 \times b^2 \times D_K \times K \quad (1)$$

$$\ln [S(b)/S(0)] = -b \times ADC \quad (2)$$

ADC was calculated for all acquired *b*-values ($ADC_{0\text{-}2000}$), and for the following selected three values: *b* = 0, 500, and 750 (s/mm^2) ($ADC_{0\text{-}500\text{-}750}$).

Statistical analysis

Statistical calculations were performed using R environment (version 3.3.2, R-Foundation, Austria) [10]. Differences at $p < 0.05$ were considered statistically significant.

Data were verified for normality of distribution using Shapiro-Wilk test. Wilcoxon rank-sum test was applied to compare DKI and ADC parameters calculated for benign and malignant liver lesions. For all parameters, ROC curves were plotted, sensitivity, specificity, and accuracy were calculated, and cut-off points were determined using Youden criterion.

Results

Significant statistical differences between benign and malignant lesions were obtained for all DKI and ADC parameters. Obtained results are shown in Table 2. Analysis of the ROC curves showed that for parameter D_K, AUC was 0.74, while for parameters K, $ADC_{0\text{-}2000}$, and $ADC_{0\text{-}500\text{-}750}$, it was 0.77, 0.77, and 0.75, respectively. The highest sensitivity (0.91) was obtained for the ADC parameter calculated on the basis of seven *b*-values (range, 0-2,000 s/mm^2). The highest specificity (0.65) was obtained for the K parameter, with the highest accuracy of 0.80. Detailed results of the ROC curve analysis are demonstrated in Table 3. These indicate that the DKI technique yields results that are statistically comparable with those using the DWI technique (Figures 1 and 2).

Table 2. Differences between benign and malignant liver lesions presented as median ± standard deviation. Bolded values for probabilities indicate differences between the two groups, achieving statistical significance

Parameter	Benign lesions	Malignant lesions	*p*-value
D_K	2.01 ± 0.75	1.53 ± 0.53	0.00015
K	0.58 ± 0.21	0.84 ± 0.25	0.000033
$ADC_{0\text{-}2000}$	1.37 ± 0.39	0.93 ± 0.25	0.000017
$ADC_{0\text{-}500\text{-}750}$	1.75 ± 0.64	1.23 ± 0.42	0.000081

Table 3. Receiver operating characteristic (ROC) curve analysis for all parameters

	D_K	K	$ADC_{0\text{-}2000}$	$ADC_{0\text{-}500\text{-}750}$
AUC	0.74	0.77	0.77	0.75
Sensitivity	0.83	0.88	0.91	0.83
Specificity	0.64	0.65	0.55	0.61
Cut-off	1.88	0.65	1.32	1.64
Accuracy	0.77	0.80	0.79	0.76

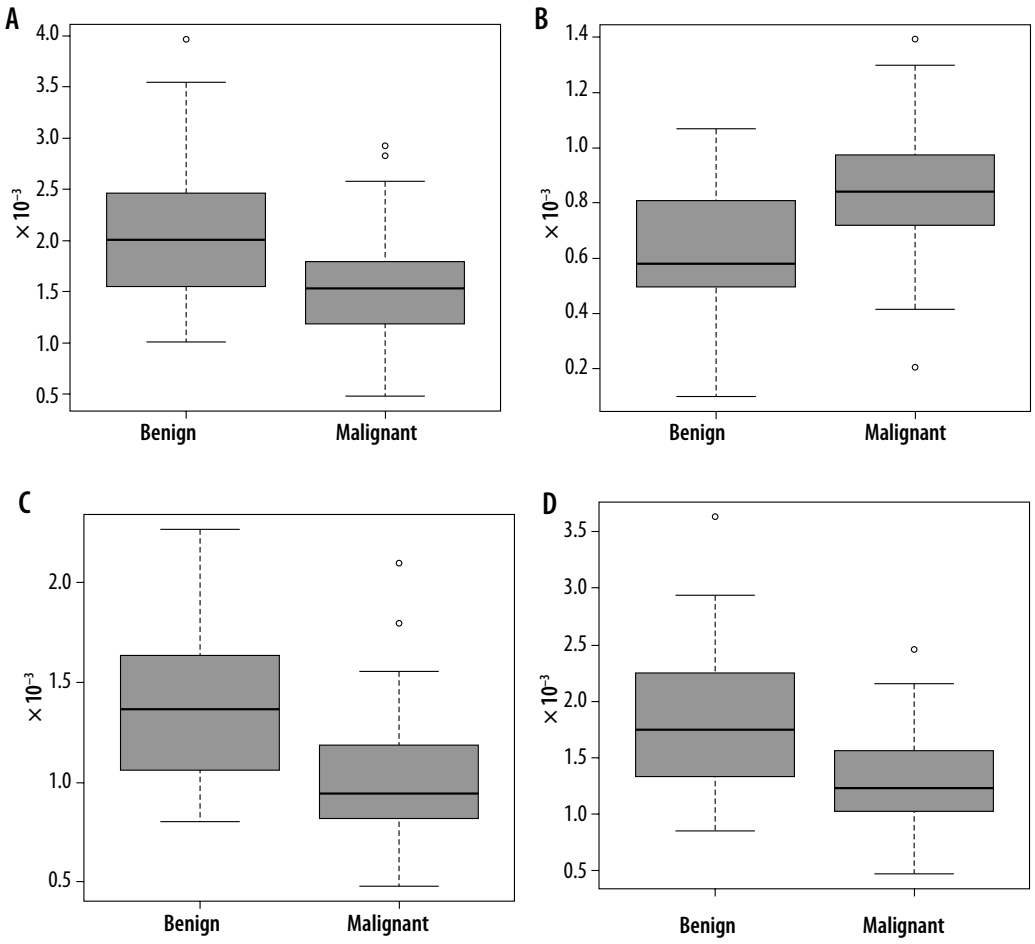

Figure 1. Box-and-whisker plots illustrate median, interquartile range, minimal and maximal, and outlier data for benign and malignant liver lesions: (**A**) D_K, (**B**) K, (**C**) $ADC_{0\text{-}2000}$, (**D**) $ADC_{0\text{-}500\text{-}700}$

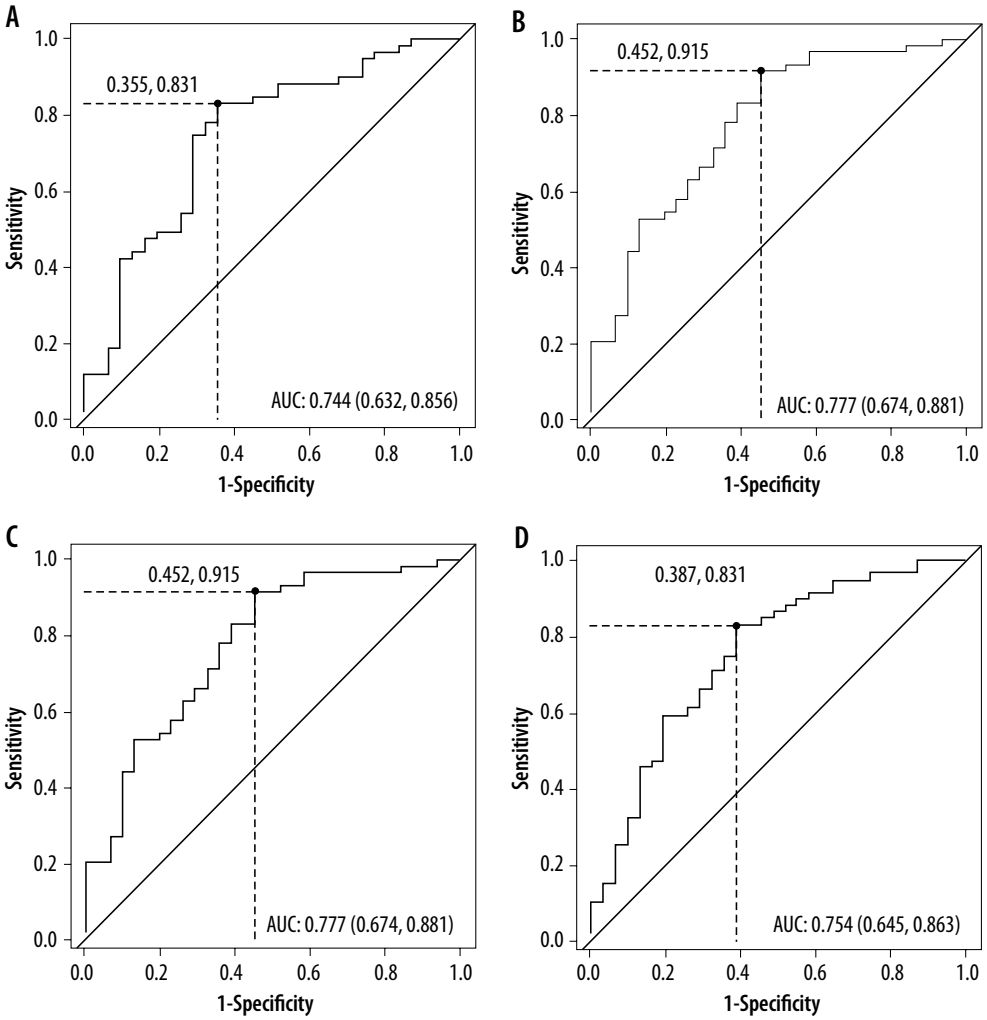

Figure 2. Receiver operating characteristic (ROC) curves. Comparisons of (**A**) D_K, (**B**) K, (**C**) $ADC_{0\text{-}2000}$, and (**D**) $ADC_{0\text{-}500\text{-}700}$ between benign and malignant liver lesions

Discussion

In the current study, ADC and DKI parameters were investigated for their ability to differentiate between malignant and benign lesions of the liver (Figure 3). All the parameters showed significant differences; however, K and ADC calculated for seven b-values achieved the greatest accuracy. D_K and ADC calculated for three *b*-values demonstrated a slightly worse performance. DKI reflects the deviation from a Gaussian distribution to characterize tissue diffusion. It is used increasingly more replacing conventional DWI for more accurate provision of information on tissue characteristics.

However, the number of studies, in which this method has been used within the liver, remains relatively small. Our results are consistent with those obtained by Jia *et al.*, who showed that ADC- and DKI-derived parameters K and D were able to distinguish HCC from FNH, hemangioma, and HCA, even as there was no evidence for D or K being superior to ADC [4]. Different from our work, metastases were not included in that study group.

While our study included seven *b*-values, with 2,000 s/mm^2 being the highest applied, there have also been attempts to obtain DKI data from a standard DWI protocol, with *b*-values of maximum 1,000 s/mm^2. In such a setting, Bujdan *et al.* found no additional value of DKI over ADC regarding the difference between benign and malignant liver lesions [8]. Interestingly, cysts and hemangiomas were included in that study, while metastases were not. Based on the results of other studies and our previous experience, we presume that acquisition of *b*-values greater than 1,000 is necessary for DKI data to be obtained, which is time-consuming due to necessity of a significantly greater number of signal averages used in case of high values. However, by reducing and selecting appropriate *b*-values, the sequence time can to shorter [11].

Most studies performed in this field considered HCC and liver fibrosis. Goshima *et al.* compared DKI and DWI to assess the viability of HCC following loco-regional treatment, and demonstrated that sensitivity, specificity, and AUC values were all superior with K than ADC. In contrast, ADC was observed to be more useful in

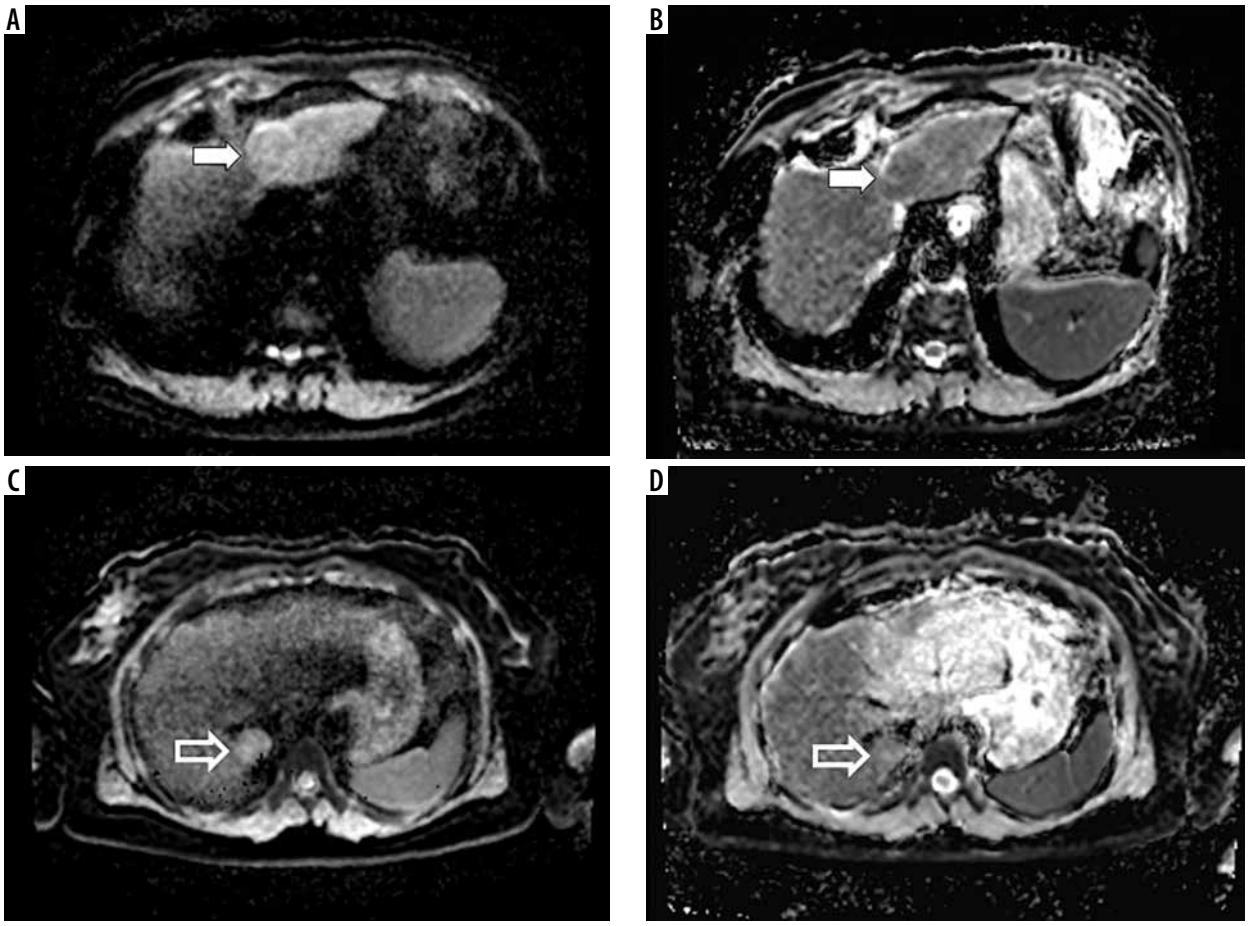

Figure 3. ADC maps created with different sets of *b*-values, $ADC_{0\text{-}500\text{-}700}$ and $ADC_{0\text{-}2000}$. Images (**A**) and (**B**) present hepatocellular carcinoma located in the left liver lobe (white arrow), and images (**C**) and (**D**) show focal nodular hyperplasia located in the posterior part of the right liver lobe (open arrow)

assessing liver parenchyma [6]. Wang *et al.* found K useful in the detection of micro-vascular involvement of HCC [5]. In a study by Cao *et al.*, K proved capable of offering moderate diagnostic efficacy (AUC = 0.77) in the recognition of micro-vascular invasion, while compared with ADC, there was a greater specificity in the identification of tumor grade [7]. Regarding liver fibrosis, Yoon *et al.* reported that K exhibited significantly greater values in clinically significant fibrosis, while ADC failed to show statistically significant differences [12]. Similar conclusions were drawn by Yoshimaru *et al.*, who demonstrated how K and D derived from DKI correlated significantly with the extent of hepatic fibrosis staging. In this study, ADC showed significant differences between cirrhotic and non-cirrhotic groups of patients, despite no capacity to differentiate between particular stages of the fibrosis [13]. Likewise, Xie *et al.* found that D derived from DKI differed from ADC in correlating better with liver fibrosis stages [14]. Zhang *et al.*, who investigated liver metastatic disease showed that low pretreatment ADC and D_K as well as high K are independent factors associated with a good response to chemotherapy in colorectal liver metastasis. Among all the parameters tested, ADC exhibited the greatest AUC and was considered the best predictive parameter [15].

In regard to benign and malignant lesions distinguished from each other in other organs, studies have confirmed the superiority of DKI over DWI, but with moderate differences. For example, in breast cancer, K and D showed significantly greater specificity than ADC (83% and 83% vs. 76%, respectively) [16], while in prostate cancer, K emerged as significantly better compared with ADC or D (93.3% vs. 78.5% and 83.5%) [17].

The present study has certain limitations. First, as there is lack of standardization of the DKI protocol, data from other studies were not readily comparable with ours. Moreover, all parameters were calculated with reference to ROI data, something that is not feasible in day-to-day practice. Comparison with data acquired through mapping would bring the results closer to clinical use. Certain examinations (in the left lobe of the liver, in particular) were impaired by motion of artefacts from the heart and diaphragm.

Finally, as the above data were all derived from a single MRI system, applicability should be verified regarding alternative MRI systems. It may be also concluded that DKI represents a further feature in the evaluation of hepatic lesions, even if our results indicate little advantage over the widely-used DWI.

Conflict of interest

The authors report no conflict of interest.

References

1. Jensen JH, Helpern JA, Ramani A, et al. Diffusional kurtosis imaging: the quantification of non-gaussian water diffusion by means of magnetic resonance imaging. Magn Reson Med 2005; 53: 1432-1440.
2. Yoon JH, Lee JM, Lee KB, et al. Comparison of monoexponential, intravoxel incoherent motion diffusion-weighted imaging and diffusion kurtosis imaging for assessment of hepatic fibrosis. Acta Radiol 2019; 60: 1593-1601.
3. Yuan ZG, Wang ZY, Xia MY, et al. Comparison of diffusion kurtosis imaging versus diffusion weighted imaging in predicting the recurrence of early stage single nodules of hepatocellular carcinoma treated by radiofrequency ablation. Cancer Imaging 2019; 19: 30.
4. Jia Y, Cai H, Wang M, et al. Diffusion kurtosis MR imaging versus conventional diffusion-weighted imaging for distinguishing hepatocellular carcinoma from benign hepatic nodules. Contrast Media Mol Imaging 2019; 2019: 2030147.
5. Wang WT, Yang L, Yang ZX, et al. Assessment of microvascular invasion of hepatocellular carcinoma with diffusion kurtosis imaging. Radiology 2018; 286: 571-580.
6. Goshima S, Kanematsu M, Noda Y, et al. Diffusion kurtosis imaging to assess response to treatment in hypervascular hepatocellular carcinoma. AJR Am J Roentgenol 2015; 204: W543-549.
7. Cao L, Chen J, Duan T, et al. Diffusion kurtosis imaging (DKI) of hepatocellular carcinoma: correlation with microvascular invasion and histologic grade. Quant Imaging Med Surg 2019; 9: 590-602.
8. Budjan J, Sauter EA, Zoellner FG, et al. Diffusion kurtosis imaging of the liver at 3 Tesla: in vivo comparison to standard diffusion-weighted imaging. Acta Radiol 2018; 59: 18-25.
9. Chernyak V, Fowler KJ, Kamaya A, et al. Liver Imaging Reporting and Data System (LI-RADS) version 2018: imaging of hepatocellular carcinoma in at-risk patients. Radiology 2018; 289: 816-830.
10. R Core Team (2016) R: A language and environment for statistical computing. R Foundation for Statistical Computing, Vienna, Austria. Available from: https://www.R-project.org/.
11. Pasicz K, Podgórska J, Jasieniak J, et al. Optimal b-values for diffusion kurtosis imaging of the liver and pancreas in MR examinations. Phys Med 2019; 66: 119-123.
12. Yoon JH, Lee JM, Kim E, et al. Quantitative liver function analysis: volumetric T1 mapping with fast multisection B(1) inhomogeneity correction in hepatocyte-specific contrast-enhanced liver MR imaging. Radiology 2017; 282: 408-417.
13. Yoshimaru D, Miyati T, Suzuki Y, et al. Diffusion kurtosis imaging with the breath-hold technique for staging hepatic fibrosis: a preliminary study. Magn Reson Imaging 2018; 47: 33-38.
14. Xie S, Li Q, Cheng Y, et al. Differentiating mild and substantial hepatic fibrosis from healthy controls: a comparison of diffusion kurtosis imaging and conventional diffusion-weighted imaging. Acta Radiol 2020; 61: 1012-1020.
15. Zhang H, Li W, Fu C, et al. Comparison of intravoxel incoherent motion imaging, diffusion kurtosis imaging, and conventional DWI in predicting the chemotherapeutic response of colorectal liver metastases. Eur J Radiol 2020; 130: 109149.
16. Sun K, Chen X, Chai W, et al. Breast cancer: diffusion kurtosis MR imaging-diagnostic accuracy and correlation with clinical-pathologic factors. Radiology 2015; 277: 46-55.
17. Rosenkrantz AB, Sigmund EE, Johnson G, et al. Prostate cancer: feasibility and preliminary experience of a diffusional kurtosis model for detection and assessment of aggressiveness of peripheral zone cancer. Radiology 2012; 264: 126-135.